DOI: 10.1002/ejic.200800591

Platinum(IV) Complexes of 3- and 4-Picolinic Acids Containing Ammine or Isopropylamine Ligands – Synthesis, Characterization, X-ray Structures, and Evaluation of Their Cytotoxic Activity against Cancer Cell Lines

María J. Macazaga,[a] Jorge Rodríguez,[a][‡] Adoración G. Quiroga,[a] Sandra Peregina,[b] Amancio Carnero,[b] Carmen Navarro-Ranninger,*[a] and Rosa M. Medina*[a]

Dedicated to Professor Jan Reedijk on the occasion of his retirement

Keywords: Platinum(IV) complexes / Platinum / Cytotoxic activity / Picolinic acids / Antitumor agents

The preparation and characterization of the new complexes *trans*-[$PtCl_4(NH_3)$(3-picolinic acid)] (**1**), *trans*-[$PtCl_4\{NH_2CH(CH_3)_2\}$(3-picolinic acid)] (**2**), *trans*-[$PtCl_4(NH_3)$(4-picolinic acid)] (**3**), and *trans*-[$PtCl_4\{NH_2CH(CH_3)_2\}$(4-picolinic acid)] (**4**) are described. The main structural feature of these complexes is the presence of ligands capable of multiple hydrogen-bonding interactions. Crystals of **1**, **2**, **3**, and **4** suitable for single-crystal X-ray diffraction were grown, and the molecular structures of these compounds are discussed. In contrast to the inactive parent Pt^{II} complexes, the Pt^{IV} complexes displayed cytotoxic activity against various cancer cell lines used at the National Cancer Institute (NCI) for in vitro screens. Once more, the isopropylamine derivatives showed the best cytotoxicity values.

Introduction

Cisplatin, named recently *cis*-diamminedichloridoplatinum(II), is known to be an anticancer drug that is particularly effective against solid tumor types, such as testicular, ovarian, head, and neck cancers, and additionally against small-cell lung cancer.[1] Quite severe side effects of cisplatin treatment together with the resistance of tumor cells to this drug have stimulated research in the development of improved platinum drugs and consequently enhanced the understanding of the molecular mechanisms that underlie the biological efficacy of platinum compounds. Brabec et al.[2] support the view that changes in the structure of platinum drugs, resulting in a DNA binding mode fundamentally different from that of "classical" cisplatin, will alter resistance pathways of platinum drugs and may also modulate their pharmacological properties.

From the beginning of research in platinum anticancer drugs, the *cis* configuration has been considered to be potentially critical for activity and has dominated drug development in this field. However, several new complexes with *trans* geometry that exhibit cytotoxicity in tumor cells have been identified.[3–6] Transplatin is more reactive than cisplatin therefore, undesired reactions on its way to the target are likely to contribute to the lack of anticancer activity. Farrell argued that the antitumor activity of *trans* complexes could be increased by using sterically demanding carrier ligands, which reduce the rate of displacement of the chlorido ligands. The formal replacement of one or both NH_3 ligands in transplatin by planar amines, such as pyridine, thiazole, quinoline, and ligands like iminoether or aliphatic amines, greatly enhances the cytotoxicity of the *trans* geometry.[3,7]

Platinum(IV) complexes have potential as anticancer agents in terms of both high activity and low toxicity.[8,9] An important question is whether such compounds are reduced before entering inside the cell, or perhaps not at all. Hambley and Hall reviewed the investigations in Pt^{IV} antitumor compounds since Barnett Rosenberg first noted the activity of such compounds. The chemical and pharmacological properties of these drugs are discussed, and both the reactions with individual biomolecules and the characterization of biotransformation products from animal and clinical trials are reviewed.[8]

[a] Inorganic Chemistry Department, Universidad Autónoma de Madrid,
Francisco Tomás y Valiente, 7. Madrid, Spain
Fax: +34-914-974-833
E-mail: carmen.navarro@uam.es
rosam.medina@uam.es
[b] Experimental Therapeutics Program, Centro Nacional de Investigaciones Oncológicas,
Madrid, Spain
[‡] Current address: School of Chemistry, Bristol University, Bristol, UK
Supporting information for this article is available on the WWW under http://www.eurjic.org or from the author.

The hydrogen bond has long been well-known to play a pivotal role in controlling self-assembly processes in numerous biological systems. In contrast, metal-containing hydrogen-bond donors and acceptors have only recently been explored as a means of assembling multidimensional arrays.[10,11] Recently, Rendina, Stang, and co-workers have reported the hydrogen-bond-mediated self-assembly of discrete and polymeric arrays from platinum(II) complexes containing nicotinamide, nicotinic acid or isonicotinic acid.[12–14]

Herein, we describe the synthesis and structures of Pt^{IV} complexes: *trans*-[$PtCl_4$L(3-picolinic acid)] [L = NH_3 (**1**); isopropylamine (**2**)] and *trans*-[$PtCl_4$L(4-picolinic acid)] [L = NH_3 (**3**); isopropylamine (**4**)], bearing ligands capable of multiple hydrogen-bonding interactions. We also describe that the mode of association between the molecules for the Pt^{IV} complexes, with isopropylamine ligands (**2** and **4**) differ remarkably in the solid state from those of the Pt^{IV} complexes with ammine ligands (**1** and **3**, as shown in Table 2). Cytotoxicity data are also presented for the following cell lines: MCF7, SF268, and NCI H460. The cell lines used include examples of adenocarcinoma from the human mammary gland (MCF7), human large-cell lung cancer (NCI H460), and central nervous system epithelial cancer (SF268). The tumor cell lines are also used at the NCI to identify novel potential anticancer drugs. Platination was studied in the MCF7 cell line.

Results and Discussion

Chemistry

In a previous publication, we reported the synthesis of Pt^{II} complexes *trans*-[$PtCl_2$L(4-picolinic acid)] and *trans*-[$PtCl_2$L(3-picolinic acid)] (L = NH_3, isopropylamine).[15] The 4-picolinic acid complexes were isolated by following the known procedure, in which the difference between the *trans* effects of halide and amine ligands is used (i.e., $Cl^- >$ amine) to achieve control of stereochemistry. The complexes with 3-picolinic acid afforded a complicated mixture, where the desired complexes were a minor product. Operating with *cis*-[$PtI_2(NH_3)_2$] as starting material, dmf as solvent, and a *cis*-[$PtI_2(NH_3)_2$]/HCl ratio of 1:10, the yield of the 3-picolinic acid complexes was higher, but still these reactions led to the formation of a mixture of the Pt^{II} and Pt^{IV} complexes (Scheme 1). This difficulty was finally overcome when hydrazine was used as reducing agent. The Pt^{II} complexes were isolated as the sole complex.

It was clear that complexes *trans*-[$PtCl_2(NH_3)$(3-picolinic acid)] and *trans*-[$PtCl_2\{NH_2CH(CH_3)_2\}$(3-picolinic acid)] undergo facile redox reactions in aqueous solution. We, and other authors, have observed this kind of novel chemistry for some *trans* complexes,[16,17] but neither the conditions nor the mechanism of the oxidation in water solution have been established. Herein, we have followed the reactions until the best conditions to isolate the Pt^{IV} complexes were obtained (Scheme 1).

The oxidation of the Pt^{II} complexes takes place in the last step, the reaction of *cis*-[PtL'_2L_2]$^{2+}$ with HCl/H_2O, since the detailed study of the ^{195}Pt NMR spectra of the products formed in the preceding steps showed only chemical shifts corresponding to Pt^{II} complexes. Then, we focused on the variation of the reaction conditions with HCl/H_2O, and when the PtI_2L_2/HCl ratio was changed from 1:10 to 1:30 (Scheme 1), only the Pt^{IV} complexes **1** and **2** were obtained. When 4-picolinic acid was used as ligand under these reaction conditions, the results were similar and led to **3** and **4**.

The reduction of complexes **1**, **2**, **3**, and **4** with $N_2H_4{\cdot}H_2O$ yields the Pt^{II} counterpart complexes. The Pt^{IV} complexes are also slowly reduced to Pt^{II} on standing in ethanol.

The four compounds have been characterized by elemental analysis and ^{1}H, ^{13}C, and ^{195}Pt NMR spectroscopy (see Experimental Section). In addition, the crystal structures have been determined. The assignment of NMR spectra was carried out in accordance with published data[15,18,19] and ^{1}H-^{195}Pt HMBC and ^{1}H-^{13}C HMQC experiments (see Experimental Section and Scheme 2). Perhaps, the ^{1}H NMR spectra of **1** and **2** are noteworthy, because of their unusual couplings. For complexes **1** and **2**, the pyridyl H_3 proton appears as a doublet of a doublet of a doublet, ddd, ($^3J_{HH}$ = 6.0 Hz, $^4J_{HH}$ = 1.1 Hz) and the H_7 proton appears as a multiplet. These signals are flanked by ^{195}Pt satellites (I = 1/2; natural abundance = 33.8%) with $^3J_{PtH}$ = 25–27 Hz. The H_5 proton appears as a ddd ($^3J_{HH}$ = 8.0 Hz, $^4J_{HH}$ = 1.5–1.3 Hz) and the H_4 proton gives rise to a multiplet. For **1** and **3**, the NH_3 protons are split into three peaks by the ^{14}N nucleus (I = 1; natural abundance = 99.6%) with J^{14}_{NH} = 53.7 Hz, and these signals are flanked by ^{195}Pt satellites with $^2J_{PtH}$ = 26.05 Hz and 26.8 Hz, respectively (Figure 1). In addition, from a ^{1}H-^{15}N HSQC experiment the $J_{15N–195Pt}$ = 261.2 Hz is obtained for **1**.

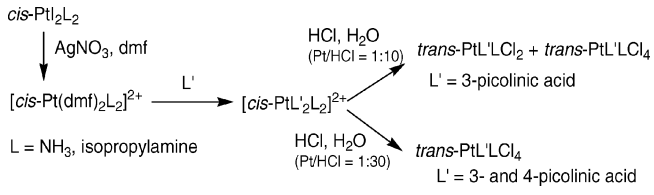

Scheme 1.

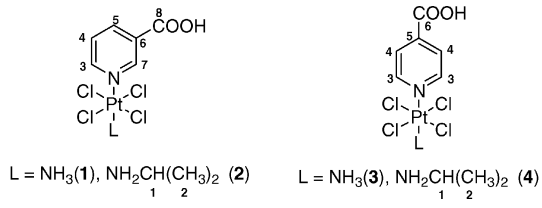

Scheme 2.

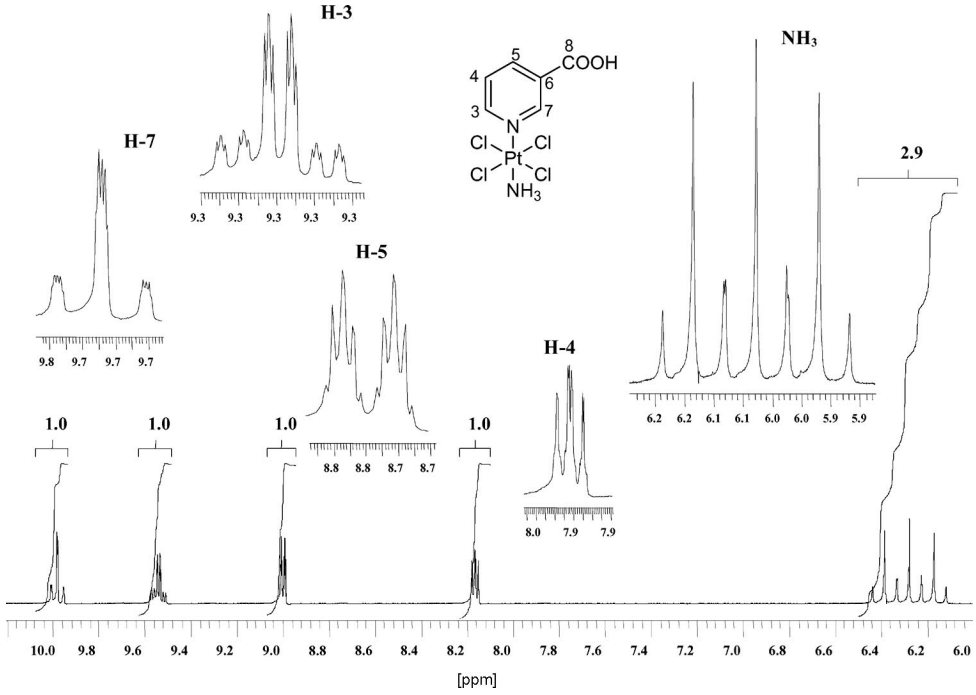

Figure 1. Atom-numbering scheme and ^{1}H NMR spectrum for complex **1**.

X-ray Structures of Complexes 1, 2, 3, and 4

Selected bond lengths [Å] and angles [°] for complexes **1**, **2**, **3**, and **4** are summarized in Table 1. The molecular structures are shown in Figure 2, Figure 3, Figure 4, and Figure 5, respectively.

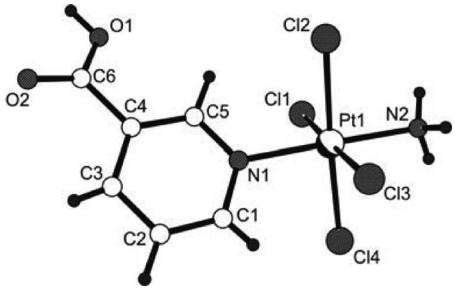

Figure 2. ORTEP diagram of **1**.

Complexes **1**, **2**, **3**, and **4** crystallize in the monoclinic system, with space groups $P2_1/c$ and $C2/c$. The ammine derivatives, **1** and **3**, crystallize as monohydrates. The Pt atom is coordinated octahedrally with angles very close to the expected values of 90° and 180°. The Pt–N (amine), Pt–N (picolinic acid) and Pt–Cl bond lengths are in agreement with published data[20,21] for Pt^{IV} complexes and are similar to those in the Pt^{II} counterparts.[15] The N–Pt–N–C(pyridine ring) torsion angles in ammine complexes **1** and **3** are 133(26)° and 166(6)°, respectively, and the carboxyl group deviations from the pyridine ring are about 25°. In the isopropylamine derivatives **2** and **4**, the torsion angles are smaller, 65(3)° and 46(3)°, respectively, and the carboxyl group deviations, about 18.5°, are slightly lower.

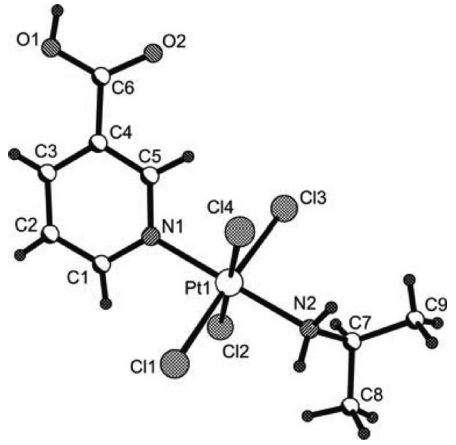

Figure 3. ORTEP diagram of **2**.

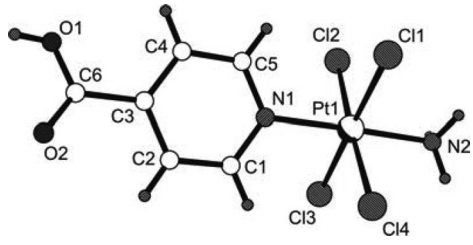

Figure 4. ORTEP diagram of **3**.

Comparing the structures of these four complexes, we observed no significant differences in the geometric parameters defining the structures of the ammine and the isopropylamine derivatives, but the mode of intermolecular association is quite distinct. In **1** and **3**, the molecules are associ-

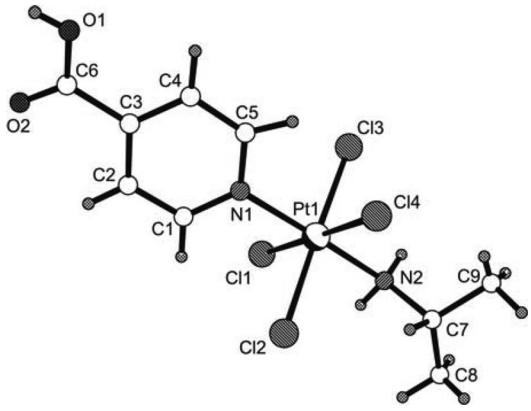

Figure 5. ORTEP diagram of **4**.

Table 1. Selected bond lengths [Å] and angles [°] for complexes **1**–**4**.

1		**3**	
Pt(1)–N(2)	2.02(3)	Pt(1)–N(2)	2.037(4)
Pt(1)–N(1)	2.06(2)	Pt(1)–N(1)	2.051(4)
Pt(1)–Cl(2)	2.308(6)	Pt(1)–Cl(4)	2.3048(1)
Pt(1)–Cl(3)	2.310(6)	Pt(1)–Cl(3)	2.3117(1)
Pt(1)–Cl(1)	2.320(6)	Pt(1)–Cl(1)	2.3117(1)
Pt(1)–Cl(4)	2.323(6)	Pt(1)–Cl(2)	2.3289(1)
N(1)–Pt(1)–N(2)	178.2(8)	N(2)–Pt(1)–N(1)	178.60(1)
N(2)–Pt(1)–Cl(2)	88.2(8)	N(2)–Pt(1)–Cl(4)	86.99(14)
N(1)–Pt(1)–Cl(2)	92.1(7)	N(1)–Pt(1)–Cl(4)	91.78(13)
N(2)–Pt(1)–Cl(3)	87.9(6)	N(2)–Pt(1)–Cl(3)	88.62(11)
N(1)–Pt(1)–Cl(3)	90.3(5)	N(1)–Pt(1)–Cl(3)	90.74(10)
Cl(2)–Pt(1)–Cl(3)	90.7(2)	Cl(4)–Pt(1)–Cl(3)	90.62(4)
N(2)–Pt(1)–Cl(1)	89.5(6)	N(2)–Pt(1)–Cl(1)	90.41(11)
N(1)–Pt(1)–Cl(1)	92.3(5)	N(1)–Pt(1)–Cl(1)	90.23(10)
Cl(2)–Pt(1)–Cl(1)	89.8(2)	Cl(4)–Pt(1)–Cl(1)	89.46(4)
Cl(3)–Pt(1)–Cl(1)	177.4(2)	Cl(3)–Pt(1)–Cl(1)	179.02(4)
N(2)–Pt(1)–Cl(4)	88.5(8)	N(2)–Pt(1)–Cl(2)	89.49(14)
N(1)–Pt(1)–Cl(4)	91.3(7)	N(1)–Pt(1)–Cl(2)	91.74(13)
Cl(2)–Pt(1)–Cl(4)	176.5(2)	Cl(4)–Pt(1)–Cl(2)	176.48(4)
Cl(3)–Pt(1)–Cl(4)	90.1(2)	Cl(3)–Pt(1)–Cl(2)	89.21(4)
Cl(1)–Pt(1)–Cl(4)	89.2(2)	Cl(1)–Pt(1)–Cl(2)	90.66(4)
2		**4**	
Pt(1)–N(2)	2.054(3)	Pt(1)–N(1)	2.058(5)
Pt(1)–N(1)	2.059(3)	Pt(1)–N(2)	2.066(5)
Pt(1)–Cl(2)	2.3062(1)	Pt(1)–Cl(2)	2.3097(15)
Pt(1)–Cl(1)	2.3139(1)	Pt(1)–Cl(4)	2.3125(13)
Pt(1)–Cl(4)	2.3161(9)	Pt(1)–Cl(3)	2.3184(14)
Pt(1)–Cl(3)	2.3188(1)	Pt(1)–Cl(1)	2.3226(13)
N(2)–Pt(1)–N(1)	177.16(13)	N(2)–Pt(1)–N(1)	175.95(19)
N(2)–Pt(1)–Cl(2)	92.76(11)	N(1)–Pt(1)–Cl(2)	92.00(14)
N(1)–Pt(1)–Cl(2)	89.96(9)	N(2)–Pt(1)–Cl(2)	88.20(17)
N(2)–Pt(1)–Cl(1)	87.85(12)	N(1)–Pt(1)–Cl(4)	89.35(13)
N(1)–Pt(1)–Cl(1)	91.32(9)	N(2)–Pt(1)–Cl(4)	94.69(15)
Cl(2)–Pt(1)–Cl(1)	90.55(5)	Cl(2)–Pt(1)–Cl(4)	90.37(6)
N(2)–Pt(1)–Cl(4)	86.99(11)	N(1)–Pt(1)–Cl(3)	89.88(14)
N(1)–Pt(1)–Cl(4)	90.29(9)	N(2)–Pt(1)–Cl(3)	89.93(17)
Cl(2)–Pt(1)–Cl(4)	179.65(4)	Cl(2)–Pt(1)–Cl(3)	178.12(5)
Cl(1)–Pt(1)–Cl(4)	89.20(4)	Cl(4)–Pt(1)–Cl(3)	89.69(5)
N(2)–Pt(1)–Cl(3)	89.41(12)	N(1)–Pt(1)–Cl(1)	89.64(13)
N(1)–Pt(1)–Cl(3)	91.39(9)	N(2)–Pt(1)–Cl(1)	86.32(16)
Cl(2)–Pt(1)–Cl(3)	89.92(5)	Cl(2)–Pt(1)–Cl(1)	89.39(5)
Cl(1)–Pt(1)–Cl(3)	177.24(4)	Cl(4)–Pt(1)–Cl(1)	178.95(5)
Cl(4)–Pt(1)–Cl(3)	90.32(4)	Cl(3)–Pt(1)–Cl(1)	90.58(5)

ated by head-to-tail [N–H···O] hydrogen-bonding interactions between the carboxyl groups and ammine ligands, which lead to the formation of infinite chains, where the adjacent pyridine-ring planes make up dihedral angles of 70.65° and 74.48°. These chains are joined in a parallel fashion by the water molecules, which are hydrogen bonded to the carboxyl groups, and an asymmetrically bifurcated hydrogen bond that involves the H(3B), which is shared by O(3), Cl(1), and Cl(4), is formed in **1** (Table 2). Hence, the overall crystal structures have a two-dimensional architecture, propagated by the water molecules. The molecules in **2** and **4** associate through the carboxylic acid dimer motif (Table 2), and in the resulting dimeric units the pyridine rings are found in parallel planes.

Table 2. Hydrogen bond lengths [Å] and angles [°] for complexes **1**–**4**.[a]

D–H···A	*d*(D–H)	*d*(H···A)	*d*(D···A)	<(DHA)
1				
O(1)–H(1D)···O(3)	0.84	1.86	2.69(3)	169.8 #1
N(2)–H(2B)···O(2)	0.91	2.40	2.87(3)	112.3 #2
O(3)–H(3B)···Cl(1)	0.8(4)	2.5(4)	3.35(2)	165(32)
O(3)–H(3B)···Cl(4)	0.8(4)	2.8(4)	3.26(2)	117(29)
2				
O(1)–H(1A)···O(2)	0.82	1.85	2.641(4)	163.1 #3
3				
N(2)–H(2A)···O(3)	0.91	2.62	3.098(6)	113.2
N(2)–H(2C)···O(2)	0.91	2.22	3.032(5)	148.3 #4
O(1)–H(1A)···O(3)	0.84	1.77	2.609(5)	177.3 #5
O(3)·····O(2)			3.208(5)	
4				
O(1)–H(1 W)···O(2)	0.77(7)	1.84(7)	2.607(6)	169(6) #6

[a] Symmetry: #1 $x + 1, y, z$; #2 $x - 1, -y + 1/2, z - 1/2$; #3 $-x + 1, -y + 2, z + 1$; #4 $x - 1, -y + 3/2, z - 1/2$; #5 $x + 1, y, z + 1$; #6 $x - 1, y, z - 1$; #7 $-x + 1, y, z$.

Biology

There are many examples of platinum(IV) complexes, but as Hambley et al. have mentioned recently,[22] there are no Pt^{IV} complexes approved for anticancer clinical treatments. The review mentioned explains the factors and the hypothesis that support the activity of Pt^{IV} complexes and justified the lack of "structure–activity" rules per se.

The study of the literature to assess the present state of knowledge on Pt^{IV} complexes manifests the need for further studies regarding the oxidation mechanism of these complexes. It has already been indicated that the purpose of this work was also the evaluation of the activity of the Pt^{IV} complexes with 3- and 4-picolinic acids in a *trans* position to the isopropylamine or ammine ligands. We additionally compare their activity with that of the precursor Pt^{II} complexes, which were published in a previous work.[15]

Platinum(IV) complex **4**, in which isopropylamine and 4-picolinic acid act as ligands, showed activity against MCF7 and SF268 but no response against NCI H460. The platinum(IV) complex **2**, in which isopropylamine and 3-pico-

linic acid act as ligands, showed only significant activity against MCF7 (Table 3). These results are interesting, especially with regard to the cytotoxic values of the precursor platinum(II) complexes which are not active.[15]

Table 3. Cytotoxic activity of the metal complexes **1**–**4**.[a]

trans-[$PtCl_4$(L′)(L)]			IC_{50} in the cell lines:		
L	L′	No.	MCF7	NCI H460	SF268
3-Picolinic acid	NH_3	**1**	NR	NR	NR
	$(CH_3)_2CH_2NH_2$	**2**	12.12	NR	NR
4-Picolinic acid	NH_3	**3**	NR	NR	NR
	$(CH_3)_2CH_2NH_2$	**4**	16.88	NR	19.17
Cisplatin			4.2	5.6	1.0

[a] IC_{50} values were determined from dose-response curves (μM) at 96 h. NR: No Response. All the compounds were tested up to 100 μM concentration.

The lipophilicity of platinum(IV) complexes has been accepted as one of the main reasons of their activation. In fact, the high cellular uptake of analogues of JM216 in vitro correlates with the high lipophilicity of the platinum(IV) complexes. In vivo, the reduction of these platinum(IV) complexes occurs so rapidly that the loss of lipophilicity probably accounts for the difference in activity between in vitro and in vivo systems.[22]

For this reason, we decided to check the platination that occurred in the DNA extracted from cells plated and inhibited with platinum(IV) complexes **1**, **2**, **3**, and **4** and compared our results with those of the corresponding platinum(II) complexes, which are not active against the cell lines checked.

Analyzing the data obtained (see Supporting Information), we observed that Pt^{IV} complexes reached the highest concentrations at 2 h. Similar results obtained with longer exposures indicate that DNA platination is a rapidly occurring event.

The higher the concentration used in the experiment, the higher the platination observed, especially for the platinum(IV) complexes, which are expected to be more lipophilic. But despite the inactivity of the Pt^{II} parent complexes, and the inactive Pt^{IV} complexes as well, platination of the DNA has taken place The platination is lower only in the case of inactive complex **1** and its Pt^{II} counterpart.. Though the values at concentrations of 10 and 50 μM seem to be higher for Pt^{IV}, the fact that values above 5 units are detected for inactive complexes, indicates that the supposed higher platination produced by a more lipophilic complex is not the main reason for the activation of the platinum(IV) complexes.

In fact, the most significant difference between active compounds **4** and **2** and inactive compounds **1** and **3**, is the presence of the isopropylamine ligand. Previous work by our group[23] and others (iproplatin in clinical trials to Phase II and III)[8] suggests that the presence of the isopropylamine ligand might produce a difference in the fashion the complexes bind to DNA, to bring about different adducts and different kinds of DNA damage, which results in different toxicity and more active complexes. Alternatively, the isopropylamine ligand might alter the disposition to react with some other cellular targets, which induces a differential response.

We think that the results presented here are interesting, and they prompt us to keep looking for differences and more targets against which this special kind of complexes may be active.

Conclusions

Several Pt^{IV} compounds have been characterized and tested against MCF7, SF268, and NCI H460 cell lines. The Pt^{IV} complexes containing isopropylamine showed cytotoxic activity against two of the cell lines: MCF7 and SF268. The crystal structures of the complexes have been solved and studied. They showed that the intermolecular associations in the solid state are different for the ammine and the isopropylamine Pt^{IV} complexes.

Experimental Section

Materials and Methods: All solvents for synthetic use were reagent grade and were used without further purification. Silver nitrate, hydrochloric acid (35%), and hydrazine hydrate ($N_2H_4{\cdot}H_2O$) were purchased from Prolabo. Dimethylformamide (dmf) (Panreac) was stored over molecular sieves (4 Å). Isopropylamine and 3- and 4-picolinic acid (Aldrich) were used without further purification. The latter two compounds were stored over P_2O_5. *cis*-[$PtI_2(NH_3)_2$] and *cis*-[$PtI_2\{NH_2CH(CH_3)_2\}$] were prepared according to published procedures.[19,24,25] The ^1H,^{13}C, and ^{195}Pt NMR spectra were recorded with a Bruker AMX-300 or 500 instrument. Chemical shifts were measured relative either to an internal reference of tetramethylsilane or to residual protons of the solvents. The reference in ^{15}N NMR spectra was liquid ammonia, and potassium hexachloridoplatinate(IV) for ^{195}Pt NMR spectroscopy. The delay used in the ^1H-^{195}Pt HMBC was 20 μs, which corresponds approximately to J = 25 Hz. Elemental analyses were performed by the Microanalytical Laboratory of the Universidad Autónoma of Madrid with a Perkin–Elmer 240 B microanalyzer. X-ray diffraction data were collected at the Monocrystal Diffraction Laboratory SIDI, Facultad de Ciencias, Universidad Autónoma of Madrid. TXRF analysis was performed by the Microanalytical Laboratory of the Universidad Autónoma of Madrid.

***trans*-[$PtCl_4(NH_3)$(3-picolinic acid)] (1):** A solution of *cis*-[$PtI_2(NH_3)_2$] (0.2108 g, 0.436 mmol) in dmf (10 mL) was treated with $AgNO_3$ (0.1482 g, 0.873 mmol) for 24 h with stirring in the dark. AgI was filtered off and 3-picolinic acid (0.1097 g, 0.873 mmol) was added to the filtrate. The reaction mixture was stirred for 5 h at 65 °C and filtered. The dmf was removed under reduced pressure and the resultant solid was treated with water (4 mL). Concentrated HCl (1.16 mL, 13.08 mmol) was added and the solution was stirred and heated to reflux for 10 h. After cooling the reaction mixture, a yellow solid was obtained. It was filtered, washed with ice-cold water and ether, and dried under vacuum. The residue obtained was extracted with cold acetone, and an insoluble white material was filtered off. The filtrate was concentrated under reduced pressure and compound **1** was obtained as a yellow solid. Yield: 0.1083 g (52%). ^1H NMR (500 MHz, [D_6]acetone, 25 °C): δ_H = 9.77 (m, $^3J_{PtH}$ = 26.4 Hz, 1 H, 7-H), 9.33 (ddd, $^3J_{HH}$ = 6.0 Hz, $^4J_{HH}$ = 1.1 Hz, $^3J_{PtH}$ = 25.2 Hz, 1 H, 3-H), 8.79 (ddd,

$^3J_{HH}$ = 8.0 Hz, $^4J_{HH}$ = 1.5 Hz, 1 H, 5-H), 7.96 (m, 1 H, 4-H), 6.08 (m, J^{14}_{NH} = 53.7 Hz, $^2J_{PtH}$ = 26.5 Hz, J^{15}_{NPt} = 130.6 Hz, 3 H, NH_3) ppm. ^{13}C NMR (75 MHz, [D$_6$]acetone, 25 °C): δ_C = 164.0 (C-8), 156.2 (C-3), 154.2 (C-7), 143.1 (C-5), 129.7 (C-6), 126.9 (C-4) ppm. ^{195}Pt NMR (107 MHz, [D$_6$]acetone, 25 °C): δ_{Pt} = –287.6 ppm. $C_6H_8Cl_4N_2O_2Pt$ (477): calcd. C 15.11, N 5.87, H 1.69; found C 15.07, N 5.86, H 1.70.

***trans*-[PtCl$_4${NH$_2$CH(CH$_3$)$_2$}(3-picolinic acid)] (2):** A solution of *cis*-[PtI$_2${NH$_2$CH(CH$_3$)$_2$}] (0.4856 g, 0.856 mmol) in dmf (10 mL) was treated with $AgNO_3$ (0.2909 g, 1.713 mmol) for 24 h with stirring in the dark. AgI was filtered off and 3-picolinic acid (0.216 g, 1.718 mmol) was added to the filtrate. The reaction mixture was stirred for 15 h at 65 °C and filtered. The dmf was removed under reduced pressure and the resultant solid was treated with water (6 mL). Concentrated HCl (2.27 mL, 25.698 mmol) was added and the solution was stirred and heated to reflux for 10 h. After cooling the reaction mixture, a yellow solid was obtained; it was filtered, washed with ice-cold water and ether, and dried under vacuum. The residue obtained was extracted with cold acetone, and an insoluble white material was filtered off. The filtrate was concentrated under reduced pressure and compound **2** was obtained as a yellow solid. Yield: 0.2550 g (57%). ^{1}H NMR (500 MHz, [D$_6$]acetone, 25 °C): δ_H = 9.75 (m, $^3J_{Pt\text{-}H}$ = 27.0 Hz, 1 H, 7-H), 9.32 (ddd, $^3J_{HH}$ = 6.0 Hz, $^4J_{HH}$ = 1.1 Hz, $^3J_{PtH}$ = 25.5 Hz,1 H, 3-H), 8.80 (ddd, $^3J_{HH}$ = 8.0 Hz, $^4J_{HH}$ = 1.3 Hz, 1 H, 5-H), 7.96 (m, 1 H, 4-H), 5.96 (s br, 2 H, NH_2), 3.67 (sp, $^3J_{HH}$ = 6.5 Hz, 1 H, 1-H), 1.56 (d, $^3J_{HH}$ = 6.5 Hz, 6 H, CH_3) ppm. ^{13}C NMR (125 MHz, [D$_6$]acetone, 25 °C): δ_C = 163.7 (C-8), 156.3 (C-3), 154.0 (C-7), 139.1 (C-5), 128.4 (C-6), 125.4 (C-4), 48.6 (C-1), 22.9 (C-2) ppm. ^{195}Pt NMR (107 MHz, [D$_6$]acetone, 25 °C): δ_{Pt} = –246.8 ppm. $C_9H_{14}Cl_4N_2O_2Pt$ (519.1): calcd. C 20.82, N 5.40, H 2.72; found C 20.80, N 5.39, H 2.72.

***trans*-[PtCl$_4$(NH$_3$)(4-picolinic acid)] (3):** A solution of *cis*-[PtI$_2$(NH$_3$)$_2$] (0.4076 g, 0.844 mmol) in dmf (10 mL) was treated with $AgNO_3$ (0.2866 g, 1.688 mmol) for 24 h with stirring in the dark. AgI was filtered off and 4-picolinic acid (0.2099 g, 1.688 mmol) was added to the filtrate. The reaction mixture was stirred for 15 h at 65 °C and filtered. The dmf was removed under reduced pressure and the resultant solid was treated with water (4 mL). Concentrated HCl (2.23 mL, 25.322 mmol) was added and the solution was stirred and heated to reflux for 20 h. After cooling the reaction mixture, a yellow solid was obtained; it was filtered, washed with ice-cold water and ether, and dried under vacuum. The residue obtained was extracted with cold acetone, and an insoluble white material was filtered off. The filtrate was concentrated under reduced pressure and compound **3** was obtained as a yellow solid. Yield: 0.0846 g (21%). ^{1}H NMR (500 MHz, [D$_6$]acetone): δ_H = 9.33 (d, $^3J_{HH}$ = 6.9 Hz, 2 H, 3-H), 8.25 (d, $^3J_{HH}$ = 6.9 Hz, 2 H, 4-H), 6.05 (m, J^{14}_{NH} = 53.7 Hz, $^2J_{PtH}$ = 26.8 Hz, 3 H, NH_3) ppm. ^{13}C NMR (125 MHz, [D$_6$]acetone): δ_C = 163.6 (C-6), 153.5 (C-3), 142.4 (C-5), 125.3 (C-4) ppm. ^{195}Pt NMR (107 MHz, [D$_6$]acetone): δ_{Pt} = –277.8 ppm. $C_6H_8Cl_4N_2O_2Pt$ (477): calcd. C 15.11, N 5.87, H 1.69; found C 15.08, N 5.86, H 1.70.

***trans*-[PtCl$_4${NH$_2$CH(CH$_3$)$_2$}(4-picolinic acid)] (4):** A solution of *cis*-[PtI$_2${NH$_2$CH(CH$_3$)$_2$}] (0.5022 g, 0.886 mmol) in dmf (10 mL) was treated with $AgNO_3$ (0.3008 g, 1.772 mmol) for 24 h with stirring in the dark. AgI was filtered off and 4-picolinic acid (0.2203 g, 1.772 mmol) was added to the filtrate. The reaction mixture was stirred for 15 h at 65 °C and filtered. The dmf was removed under reduced pressure and the resultant solid was treated with water (6 mL). Concentrated HCl (2.35 mL, 26.576 mmol) was added and the solution was stirred and heated to reflux for 20 h. After cooling the reaction mixture, a yellow solid was obtained; it was filtered, washed with ice-cold water and ether, and dried under vacuum. The residue obtained was extracted with cold acetone, and an insoluble white material was filtered off. The filtrate was concentrated under reduced pressure and compound **4** was obtained as a yellow solid. Yield: 0.2049 g (44%). ^{1}H NMR (500 MHz, [D$_6$]acetone): δ_H = 9.31 (d, $^3J_{HH}$ = 6.9 Hz, $^3J_{PtH}$ = 25.9 Hz, 2 H, 3-H), 8.24 (d, $^3J_{HH}$ = 6.9 Hz, 2 H, 4-H), 5.94 (s br, 2 H, NH_2), 3.67 (m, $^3J_{HH}$ = 6.5 Hz, 1 H, 1-H), 1.56 (d, $^3J_{HH}$ = 6.5 Hz, 6 H, CH_3) ppm. ^{13}C NMR (125 MHz, [D$_6$]acetone): δ_C = 164.4 (C-6), 154.7 (C-3), 143.4 (C-5), 126.2 (C-4), 52.1 (C-1), 23.1 (C-2) ppm. ^{195}Pt NMR (107 MHz, [D$_6$]acetone): δ_{Pt} = –246 ppm. $C_9H_{14}Cl_4N_2O_2Pt$ (519.1): calcd. C 20.82, N 5.40, H 2.72; found C 20.78, N 5.39, H 2.73.

Reduction of 1, 2, 3, and 4 with Hydrazine Hydrate ($N_2H_4{\cdot}H_2O$): A suspension of **1** (0.0742 g, 0.155 mmol) in water (2 mL) was treated with hydrazine hydrate ($N_2H_4{\cdot}H_2O$) (3.86 μL, 0.078 mmol). The reaction mixture was stirred and heated to reflux for 14 h. The solvent was evaporated under reduced pressure and the residue obtained was washed with water and dried under vacuum. The residue was extracted with acetone and concentration under reduced pressure resulted in *trans*-[PtCl$_2$(NH$_3$)(3-picolinic acid)] as a yellow solid. Yield: 0.0322 g (51%). For the other complexes, the procedure described above was used, but with **2** (0.056 g, 0.108 mmol), **3** (0.11 g, 0.230 mmol), and **4** (0.1077 g, 0.207 mmol) as reactant, which resulted in the corresponding Pt^{II} complexes as yellow solids. Yield: 0.0454 g (94%), 0.0543 g (58%), and 0.0558 g (60%), respectively.

X-ray Crystallography: Yellow crystals of **1**, **2**, **3**, and **4** were obtained by slow crystallization from a solution of the compound in acidified water with HCl and acetone. A summary of selected crystallographic data for **1**, **2**, **3**, and **4** is given in Table 4. A single crystal of approximate dimensions $0.08 \times 0.06 \times 0.03$ mm for **1**, $0.13 \times 0.06 \times 0.02$ mm for **2**, $0.06 \times 0.04 \times 0.02$ mm for **3**, and $0.25 \times 0.20 \times 0.15$ mm for **4** with prismatic shape was mounted on a glass fiber and transferred to a Bruker SMART 6 K CCD area-detector three-circle diffractometer with a MAC Science Co., Ltd. Rotating Anode (Cu-K_α radiation, λ = 1.54178 Å). The generator was equipped with Goebel mirrors at settings of 50 kV and 100 mA for **1** and **4**, 50 kV and 110 mA for **2**, and 45 kV and 110 mA for **3**.[26]

X-ray data were collected at 100 K for **1**, **3**, and **4** and at 296 K for **2**, with a combination of six runs at different ϕ and 2θ angles, with 3600 frames. The data were collected using 0.3° wide ω scans (5 s/frame at 2θ = 40° and 10 s/frame at 2θ = 100° for **1**, 10 s/frame at 2θ = 40° and 20 s/frame at 2θ = 100° for **2**, 8 s/frame at 2θ = 40° and 30 s/frame at 2θ = 100° for **3**, and 1 s/frame at 2θ = 40° and 2 s/frame at 2θ = 100° for **4**), with a crystal-to-detector distance of 4.0 cm.

The raw intensity data frames were integrated with the SAINT program,[27] which also applied corrections for Lorentz and polarization effects.

The substantial redundancy in data allows empirical absorption corrections (SADABS)[28] to be applied by using multiple measurements of symmetry-equivalent reflections (ratio of minimum to maximum apparent transmissions: 0.431147 for **1**, 0.486217 for **2**, 0.412695 for **3**, and 0.253558 for **4**). The software package SHELXTL version 6.10[29] was used for space group determination, structure solution and refinement. The structure was solved by direct methods (SHELXS-97),[30] completed with difference Fourier syntheses, and refined with full-matrix least-squares techniques by using SHELXL-97[31] to minimize $\omega(F_o^2 - F_c^2)^2$. Weighted R factors (R_w) and all goodness-of-fit S values are based

Table 4. Crystal data and structure refinement for compounds **1**, **2**, **3**, and **4**.

Compound	**1**	**2**	**3**	**4**
Empirical formula	$C_6H_{10}Cl_4N_2O_3Pt$	$C_9H_{14}Cl_4N_2O_2Pt$	$C_6H_{10}Cl_4N_2O_3Pt$	$C_9H_{14}Cl_4N_2O_2Pt$
Formula weight	495.05	519.11	495.03	519.11
Temperature [K]	100(2)	296(2)	100(2)	100(2)
Wavelength [Å]	1.54178	1.54178	1.54178	1.54178
Crystal system	monoclinic	monoclinic	monoclinic	monoclinic
Space group	$P2_1/c$	$P2_1/c$	$P2_1/c$	$C2/c$
Unit cell dimensions				
a [Å]	10.10110(1)	14.8951(6)	9.71050(10)	26.8390(5)
b [Å]	10.52380(1)	8.6160(3)	11.15180(10)	8.05580(10)
c [Å]	11.81280(10)	12.5291(5)	11.5222(2)	14.9026(2)
α [°]	90	90	90	90
β [°]	100.7460(10)	112.846(2)	96.5990(10)	113.1540(10)
γ [°]	90	90°.	90	90
Volume [Å^3]	1233.70(2)	1481.80(10)	1239.47(3)	2962.55(8)
Z	4	4	4	8
Density (calculated) [Mg/m^3]	2.665	2.327	2.642	2.328
Absorption coefficient [mm^{-1}]	29.234	24.331	29.097	24.339
$F_{(000)}$	920	976	912	1952
Crystal size [mm]	$0.08 \times 0.06 \times 0.03$	$0.13 \times 0.06 \times 0.02$	$0.06 \times 0.04 \times 0.02$	$0.25 \times 0.20 \times 0.15$
θ range for data collection [°]	4.46 to 70.56	3.22 to 70.47	4.58 to 68.21	3.58 to 70.61
Index ranges	$-12 \leq h \leq 12$, $-12 \leq k \leq 12$, $-14 \leq l \leq 13$	$-17 \leq h \leq 17$, $-10 \leq k \leq 10$, $-13 \leq l \leq 14$	$-11 \leq h \leq 10$, $-12 \leq k \leq 13$, $-13 \leq l \leq 13$	$-31 \leq h \leq 32$, $-9 \leq k \leq 9$, $-18 \leq l \leq 16$
Reflections collected	7645	9187	6912	7945
Independent reflections	2252 [R(int) = 0.0320]	2742 [R(int) = 0.0393]	2170 [R(int) = 0.0363]	2716 [R(int) = 0.0451]
Completeness to θ = 70.56°	94.9%	96.9%	95.7%	95.5%
Absorption correction	SADABS v. 2.03	semi-empirical from equivalents		SADABS v. 2.03
Refinement method		full-matrix least squares on F^2		
Data/restraints/parameters	2252/3/173	2742/0/208	2170/0/147	2716/0/211
Goodness-of-fit on F^2	1.123	1.095	1.029	1.065
Final R indices [$I > 2\sigma(I)$]	R_1 = 0.0220, wR_2 = 0.0575	R_1 = 0.0219, wR_2 = 0.0554	R_1 = 0.0251, wR_2 = 0.0661	R_1 = 0.0356, wR_2 = 0.0921
R indices (all data)	R_1 = 0.0225, wR_2 = 0.0579	R_1 = 0.0234, wR_2 = 0.0561	R_1 = 0.0284, wR_2 = 0.0681	R_1 = 0.0379, wR_2 = 0.0939
Largest diff. peak and hole [e/Å^3]	1.025 and –2.081	0.996 and –0.653	1.217 and –0.920	3.032 and –2.013

on F^2; conventional R factors (R) are based on F. All non-hydrogen atoms were refined with anisotropic displacement parameters. All scattering factors and anomalous dispersion factors are contained in the SHELXTL 6.10 program library. The hydrogen atom positions for complexes **1**, **2**, **3**, and **4** were calculated geometrically and were allowed to ride on their parent carbon atoms with fixed isotropic U or localized by their electronic densities and isotropically refined.

CCDC-621686, -621688, -691266, and -691265 for compounds **1**, **2**, **3**, and **4**, respectively, contain the supplementary crystallographic data for this paper. These data can be obtained free of charge from The Cambridge Crystallographic Data Centre via www.ccdc.cam.ac.uk/data_request/cif.

Cell Lines and Culture Conditions: The cell lines used for the experiments were adenocarcinoma from the human mammary gland (MCF7), human large-cell lung cancer (NCI H460), and central nervous system epithelial cancer (SF268). All cell lines were grown in Dubelcco's Modified Eagle's Medium (DMEM) supplemented with 10% Fetal Calf Serum (FCS), fungizone, and penicillin/streptomycin.

Assessment of Cytotoxicity: The compounds were tested on 96-well trays. Cells grown in a flask were harvested just before they became confluent, counted with a haemocytometer, and diluted down with the growth medium to adjust the concentration to the required number of cells per 0.2 mL (volume for each well). Cells were then seeded in 96-well trays at a density between 1000 and 4000 cells/well, depending on the cell size. Cells were left to plate down and grow for 24 h before the drugs were added.

Drugs were weighed out and were diluted with water to get them in solution with a concentration of 10 mM. From here, a "mother plate" with serial dilutions was prepared at 1/200th of the final concentration in the culture. The appropriate volume of the compound solution (usually 2 μL) was added automatically (Beckman FX 96 tip) to the medium to bring it to the final concentration for each drug.

The medium was removed from the cells and replaced with 0.2 mL of medium dosed with the drug. Each concentration was assayed in triplicate. A control well set with untreated cells, just before adding the drugs, was obtained (seeding control, number of cells starting the culture).

Cells were exposed to the drugs for 96 h and then washed twice with phosphate buffered saline before they were fixed with glutaraldehyde (10%). Afterwards, the cells were washed twice and fixed with crystal violet (0.5%) for 30 min. Then they were washed extensively, solubilized with acetic acid (15%) and absorbance measurements were carried out at 595 nm.

DNA Platination Assay: Adenocarcinoma cells from the human mammary gland (MCF7) were grown to 70% confluence. Then, the adequate concentration of compound was added to reach a final concentration of 10 μM, 50 μM, and 100 μM. After 2, 4, or 8 h incubation, the cells were placed on ice and lysed by hypotonic

shock. The cell extract was collected and processed with RNAse (1 μg/mL for 30 min), then, proteinase K (10 μg/mL) was added and the mixture was incubated for 2 h at 50 °C. At the end of this period, the DNA was extracted with phenol/chloroform, precipitated with sodium acetate, and resuspended in H_2O for further processing/reading Pt. The analysis with total reflection X-ray fluorescence (TXRF) was performed with a Seifert EXTRAII spectrometer (Rich. Seifert, Ahrensburg, Germany). The DNA content of each sample used in the TXRF measurements was previously determined by UV/Vis spectroscopy with a NanoDrop ND1000 tool. The analysis was carried out with the already published methodology.[32]

Supporting Information (see footnote on the first page of this article): Graphs with the platination produced by complexes **1**–**4** and their parent Pt^{II} complexes versus concentration in μM.

Acknowledgments

We express our great appreciation to the Spanish Comisión Interministerial de Ciencia y Tecnología (CICYT), Salud y Farmacia (SAF), number 2006-03296. We would like to thank Dr. Pablo Sanz for his help with the X-ray data.

[1] G. Giaccone, *Drugs* **2000**, *59*, Suppl. 4, 9–17.
[2] V. Brabec, J. Kasparkova, *Drug Resistence Updates* **2002**, *5*, 147–161.
[3] N. Farrell, *Metal Ions in Biological Systems* (Eds.: A. Sigel, H. Sigel.), Marcel Dekker, Inc., New York, **1996**, *32*, p. 603–639.
[4] J. M. Pérez, L. R. Kelland, E. I. Montero, F. E. Boxall, C. A. Fuertes, C. Navarro-Ranninger, *Mol. Pharmacol.* **2003**, *63*, 933–944.
[5] U. Kalinowska-Lis, J. Ochocki, K. Matlawska-Wasowskab, *Coord. Chem. Rev.* **2008**, *252*, 1328–1345.
[6] M. Coluccia, G. Natile, *Coord. Chem. Rev.* **2001**, *216–217*, 383–410.
[7] J. Kasparkova, V. Marini, Y. Najajreh, D. Gipson, V. Brabec, *Biochemistry* **2003**, *42*, 6321–6332.
[8] M. D. Hall, T. W. Hambley, *Coord. Chem. Rev.* **2002**, *232*, 49–67.
[9] M. R. Reithofer, S. M. Valiahdi, M. A. Jakupec, V. B. Arion, A. Egger, M. Galanski, B. K. Keppler, *J. Med. Chem.* **2007**; *50*, 6692–6699.
[10] D. Braga, F. Crepioni, G. R. Desiraju, *Chem. Rev.* **1998**, *98*, 1375–1405.
[11] A. D. Burrows, C. W. Chan, M. M. Chowdhry, J. E. McGrady, D. M. P. Mingos, *Chem. Soc. Rev.* **1995**, *24*, 329–339.
[12] N. C. Gianneschi, E. R. T. Tiekink, L. M. Rendina, *J. Am. Chem. Soc.* **2000**, *122*, 8474–8479.
[13] M. G. Crisp, E. R. T. Tiekink, L. M. Rendina, *Inorg. Chem.* **2003**, *42*, 1057–1063.
[14] C. J. Kuehl, F. M. Tabellion, A. M. Arif, P. J. Stang, *Organometallics* **2001**, *20*, 1956–1959.
[15] R. M. Medina, J. Rodríguez, A. G. Quiroga, F. J. Ramos-Lima, V. Moneo, A. Carnero, C. Navarro-Ranninger, M. J. Macazaga, *Chem. Biodiv.*, in press (October 2008).
[16] A. M. Pizarro, V. P. Munk, C. Navarro-Ranninger, P. J. Sadler, *Angew. Chem. Int. Ed.* **2003**, *42*, 5339–5342.
[17] S. Shamsuddin, M. S. Ali, S. Huang, A. R. Khokhar, *J. Coord. Chem.* **2002**, *55*, 659–665.
[18] D. P. Gallash, E. R. T. Tlekink, M. Rendina, *Organometallics* **2001**, *20*, 3373–3382.
[19] E. Pantoja, A. Alvarez-Vadés, J. M. Pérez, C. Navarro-Ranninger, J. Reedijk, *Inorg. Chim. Acta* **2002**, *339*, 525–531.
[20] S. Neidle, C. F. Snook, B. A. Murrer, C. F. J. Barnard, *Acta Crystallogr., Sect. C* **1995**, *51*, 822–824.
[21] R. Kuroda, S. Neidle, I. M. Ismael, P. J. Sadler, *Inorg. Chem.* **1983**, *22*, 3620–3624.
[22] M. D. Hall, H. R. Mellor, R. Callaghan, T. W. Hambley, *J. Med. Chem.* **2007**, *50*, 3403–3411.
[23] F. J. Ramos-Lima, O. Vrana, A. G. Quiroga, C. Navarro-Ranninger, A. Halamikova, H. Rybnickova, L. Hejmalova, V. Brabec, *J. Med. Chem.* **2006**, *49*, 2640–2651 and references cited therein.
[24] S. H. Dhara, *Ind. J. Chem.* **1970**, *8*,193.
[25] S. Grabner, B. Modec, M. Čemažar, N. Bukovec, *J. Inorg. Biochem.* **2005**, *99*, 1465–1471.
[26] *SMART* v. 5.625, *Area-Detector Software Package*, Bruker AXS **1997**–**2001**, Madison, WI.
[27] *SAINT*+ NT version 6.04, *SAX Area-Detector Integration Program*, Bruker AXS **1997**–**2001**, Madison, WI.
[28] G. M. Sheldrick, *SADABS* version 2.03, *A Program for Empirical Absorption Correction*, University of Göttingen, Göttingen, **1997**–**2001**.
[29] *Bruker AXS SHELXTL* version 6.10, *Structure Determination Package*, Bruker AXS **2000**, Madison, WI.
[30] *SHELXS-97*, *Program for Structure Solution*: G. M. Sheldrick, *Acta Crystallogr., Sect. A* **1990**, *46*, 467.
[31] G. M. Sheldrick, *SHELXL-97*, *Program for Crystal Structure Refinement*, University of Göttingen, **1997**.
[32] R. Fernández Ruiz, J. D. Tornero, V. M. González, C. Alonso, *Analyst* **1999**, *124*, 583–585.

Received: June 12, 2008
Published Online: September 11, 2008

